PROBLEMS OF MECHATRONICS
ARMAMENT, AVIATION, SAFETY ENGINEERING

ISSN 2081-5891

5, 1 (15), 2014, 9-24

Weapon Barrel and Its Additional Accessories

Peter LISÝ*, Mário ŠTIAVNICKÝ

Academy of the Armed Forces
Demänová 393, 031 06 Liptovský Mikuláš 6, Slovak Republic
**corresponding author, e-mail: Peter.Lisy@aos.sk*

Manuscript received May 15,2012. Final manuscript received July 9, 2013

Abstract. This paper deals with any additional accessories has on a weapon barrel during the initial shot this was done by numerical simulation. This means, that in this paper the influence that the configuration of the assault rifle has on its accuracy is solved. Moreover the weapons muzzle position during the firing of a shot without the influence of temperature or wear of the barrel is solved. The weapon barrel and bullet are both modelled using LS-DYNA software. The barrel is steel and is ideally straight without any structural or manufactured deviations. The bullet is NATO standard 5.56 mm calibre which is consists of a brass jacket and a lead core. The bullets interaction with the barrel during a shot is given by pressured gunpowder gasses both in the barrel and the bullets base whereby it gives the bullet its forward velocity. At the initial stages of the bullets flight it has to overcome its engraving into grooves of the barrel. Both applied pressure and the movement of the bullet along the barrel gives rise to barrel vibration. This barrel vibration has an influence on its muzzle position when the bullet leaves the muzzle. Furthermore, both additional accessories and various conditions of the barrels grip onto the weapons casing have additional influences on the muzzles position when the bullet leaves the muzzle, thus having a great influence on precision

Keywords: assault rifle, weapon barrel vibration, numerical simulation

This paper is based on the work presented at the 9th International Armament Conference on „Scientific Aspects of Armament and Safety Technology", Pułtusk, Poland, September 25-28, 2012.

1. INTRODUCTION

In this paper barrel vibration which is one of the key factors that can affect the accuracy of a weapon is solved, this was done by numerical simulation. There are many variables which affect rifles accuracy [1, 2, 3 and 4]. When a weapon is fired, vibrations are induced in the steel barrel as the bullet has to overcome engraving into the grooves inside of the bore barrel and also the bullets is movement through the barrel [5]. The first investigation will be done on a simple cone-shaped barrel without any additional accessories and also with three different grippings around the chamber. The next will be three exact barrels the same as the simple cone-shaped barrel, but with additional accessories also with three different grippings. These additional accessories simulate added weight onto the barrel and muzzle (e.g. bayonet, foresight, muzzle break etc.) and also there is added weight of the gas attachment (Fig. 1).

Fig. 1. Assault rifle with the additional accessories on its barrel [6]

All of these things will be investigated mainly for the barrel and muzzle position when the bullet leaves as the barrel and muzzle position has a significant influence on the bullets flight path.

2. METHOD OF SOLUTION

In a standard three-dimensional case for dynamic analysis to solve the problems are described by a harmonic equation containing spatial derivatives of unknown function θ as follows [7]:

$$\frac{\partial}{\partial x}\left(k\frac{\partial\theta}{\partial x}\right)+\frac{\partial}{\partial y}\left(k\frac{\partial\theta}{\partial y}\right)+\frac{\partial}{\partial z}\left(k\frac{\partial\theta}{\partial z}\right)=\rho\frac{\partial^2\theta}{\partial t^2}+c\frac{\partial\theta}{\partial t}-Q \tag{1}$$

where k is the stiffness of the structure, Q is the external load applied to the structure and c and ρ are damping and mass density properties of the material respectively. The unknown function is a function of the space coordinates and of time whereas the structural and material properties are the functions of space, time and functions of an unknown quantity for nonlinear problems.

In order to solve such equations by numerical means it is required for the problem to be discretized onto finite elements. That means that space discretization where the unknown quantity in any one point in the structure domain can be approximated by the shape functions N_i from the nodal values u_i:

$$\theta = \sum N_i u_i = \mathbf{Nu} \tag{2}$$

The linear eight node brick elements were used in the model with the corresponding linear shape functions of the parametric coordinates (ξ, η, ζ) [8]:

$$N_i = \frac{1}{8}(1+\xi\xi_i)(1+\eta\eta_i)(1+\zeta\zeta_i) \tag{3}$$

where ξ_i, η_i, ζ_i are natural coordinates of i-th node. One point of the gauss integration was performed for the constant stress in element volume.

Denoting the right side in Eq. (1) by p, the total force acting on the structure can be derived using the shape functions as:

$$\mathbf{p} = \int_V \mathbf{N}^T \left(\rho \frac{\partial^2 \theta}{\partial t^2} + c \frac{\partial \theta}{\partial t} - Q\right) \mathrm{d}V \tag{4}$$

Furthermore, according to Eq. (2), the unknown variable θ can be approximated in terms of the nodal values $\boldsymbol{u}$:

$$\mathbf{p} = \left(\int_V \mathbf{N}^T \rho \mathbf{N} \mathrm{d}V\right) \frac{\mathrm{d}^2 u}{\mathrm{d}t^2} + \left(\int_V \mathbf{N}^T c \mathbf{N} \mathrm{d}V\right) \frac{\mathrm{d}u}{\mathrm{d}t} - \int_V \mathbf{N}^T Q \mathrm{d}V \tag{5}$$

The left side of the Eq. (1) leads to a formulation of the stiffness matrix in the terms of the shape function derivations which are expressed as a strain matrix **B**:

$$\mathbf{B} = [\mathbf{B}_1 \ \mathbf{B}_2 \ \mathbf{B}_3 \ \mathbf{B}_4 \ \mathbf{B}_5 \ \mathbf{B}_6 \ \mathbf{B}_7 \ \mathbf{B}_8] \tag{6}$$

where

$$\mathbf{B}_i = \begin{bmatrix} \frac{\partial N_i}{\partial x} & 0 & 0 \\ 0 & \frac{\partial N_i}{\partial y} & 0 \\ 0 & 0 & \frac{\partial N_i}{\partial z} \\ 0 & \frac{\partial N_i}{\partial z} & \frac{\partial N_i}{\partial y} \\ \frac{\partial N_i}{\partial z} & 0 & \frac{\partial N_i}{\partial x} \\ \frac{\partial N_i}{\partial y} & \frac{\partial N_i}{\partial x} & 0 \end{bmatrix} \tag{7}$$

Thus the stiffness matrix **K** can be formulated, and also as previously the mass matrix **M** and damping matrix **C** are obvious, as is the external force vector **f**:

$$\begin{aligned}\mathbf{K} &= \int_V \mathbf{B}^T\mathbf{D}\mathbf{B}\mathrm{d}V \\ \mathbf{M} &= \int_V \mathbf{N}^T\rho\mathbf{N}\mathrm{d}V \\ \mathbf{C} &= \int_V \mathbf{N}^T c\mathbf{N}\mathrm{d}V \\ \mathbf{f} &= \int_V \mathbf{N}^T Q\mathrm{d}V\end{aligned} \tag{8}$$

where **D** is a material constants for isotropic materials:

$$\mathbf{D} = \begin{bmatrix} \frac{E(1-\nu)}{(1-2\nu)(1+\nu)} & \frac{E\nu}{(1-2\nu)(1+\nu)} & \frac{E\nu}{(1-2\nu)(1+\nu)} & 0 & 0 & 0 \\ \frac{E\nu}{(1-2\nu)(1+\nu)} & \frac{E(1-\nu)}{(1-2\nu)(1+\nu)} & \frac{E\nu}{(1-2\nu)(1+\nu)} & 0 & 0 & 0 \\ \frac{E\nu}{(1-2\nu)(1+\nu)} & \frac{E\nu}{(1-2\nu)(1+\nu)} & \frac{E(1-\nu)}{(1-2\nu)(1+\nu)} & 0 & 0 & 0 \\ 0 & 0 & 0 & G & 0 & 0 \\ 0 & 0 & 0 & 0 & G & 0 \\ 0 & 0 & 0 & 0 & 0 & G \end{bmatrix} \tag{9}$$

E, *v* and *G* are Young's modulus, Poisson's ratio and shear modulus respectively.

After the discretization equation (1) can be written in a matrix form which gives the differential equation for dynamic motion:

$$\mathbf{M}\ddot{\mathbf{u}} + \mathbf{C}\dot{\mathbf{u}} + \mathbf{K}\mathbf{u} = \mathbf{f} \tag{10}$$

where the letter marked with a dot means the temporal derivation. The temporal discretization is solved by forwarding the solution from the initial conditions by the central difference method. That means that as soon as the accelerations are known, the velocity and displacement is stepped using the values from the last step as follows:

$$\begin{aligned} v_{i+1/2} &= v_{i-1/2} + a_i\Delta t_i \\ u_{i+1} &= u_i + v_{i+1/2}\Delta t_{i+1/2} \end{aligned} \tag{11}$$

where

$$\Delta t_{i+1/2} = \frac{\Delta t_i + \Delta t_{i+1}}{2} \tag{12}$$

is nodal value in *i*-th cycle.

3. NUMERICAL SIMULATION BY LS-DYNA

For solving the problem of the interaction between the bullet and all of the modifications of the cone-shaped barrels 3-D models were created using LS-DYNA software [9].

The models incorporate the simple weapon barrel for the cartridge 5.56 mm NATO with a rifling twist rate of 1:9 and exact barrels with their added accessories. The barrels material and additional accessories are from steel (Young's modulus $E = 2.07 \cdot 10^5$ MPa, Poisson's ratio $\mu = 0.3$ and specific mass density $\rho = 7830$ kg·m^{-3}). The bullet is composed of a brass jacket and a lead alloy core. The barrel bore consists of 46 rings along the length in order to obtain an accurate model loading the barrel by pressure gunpowder gasses. The simple cone-shaped barrel is quite close to the real barrel, i.e. its length is 488 mm, the outer part around the barrel chamber is cylindrical (25×60 mm) and the next part the muzzle is conical (with an outer diameter of 17 mm). Gripping (boundary condition) both on the bottom of the barrel and around the cylindrical rear part of the barrel is applied.

On the barrel bore and base of the bullet we applied a curve of time dependence of the gunpowder gasses pressure, where this curve was obtained by ballistic measurement. The interaction between the barrel bore and bullet through the automatic-surface-to-surface contact of active segments was solved. The rifling of the barrel bore is composed of six lands and six grooves and through defined conditions contact, the bullet has to overcome engraving into grooves of the barrel as in a real barrel. The barrel, its accessories and bullet mode were created with 8-node hexahedral solid elements. The full model has 61 400 solid elements and 69 874 nodes. The simple cone-shaped barrel has 23 760 nodes and the bullet has 41 632 nodes. The doubling in the precision of version LS-DYNA was used and corresponding results were under two and half per cent correct.

Figure 2 shows a simple cone-shaped barrel model with the number of node being 10 648 directly on the barrels muzzle, i.e. on the last node which is on the edge of the left land side. It also shows the bullet after 1 ms simulation with the number of node being 26 703 which is situated directly at the centre of the bullet base. It is clear see the engraved grooves on the jacket of the bullet.

All results listed in Table 1 are of a simulation time of 0.7765 when the bullet base leaves the barrel muzzle. These results with three different grippings around the chamber (20 mm, 40 mm and 60 mm) for the simple cone-shaped barrel and cone-shaped barrels with additional accessories or added weight (1 – 5×30 twice; 2 – 5×30 and 6×100; 3 – 5×20 twice and 6×100; all dimensions in mm) were obtained. Table 1 lists displacements of the barrel muzzle in x, y, z-axis and results of acceleration both at node 10 648 and the displacements of the bullet base in x, y-axis at node 26 703.

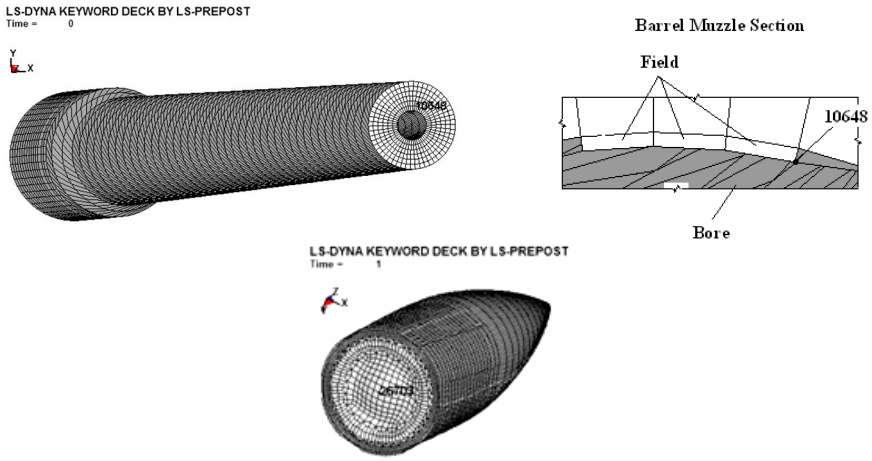

Fig. 2. Cone-shaped barrel (node 10 648) and bullet (node 26 703) at time of simulation 1 ms

Table 1. Results of displacements and acceleration at node 10 648 and displacements at node 26 703

Barrel (accessories)	Grip-ping [mm]	Displacement Node 10 648			Resultant Acceleration Node 10 648	Displacement Node 26 703	
		x	*y*	*z*		*x*	*y*
		$\cdot 10^3$ [mm]	$\cdot 10^3$ [mm]	$\cdot 10^3$ [mm]	$\cdot 10^{-3}$ [mm.ms^{-2}]	$\cdot 10^3$ [mm]	$\cdot 10^3$ [mm]
Cone-shaped	20	-5.79	10.21	4.48	14.21	-5.23	14.69
Cone-shaped	40	-4.09	5.48	4.48	198.97	1.49	-3.99
Cone-shaped	60	-6.91	13.19	4.08	45.56	3.37	-4.57
Cone-shaped (1)	20	-7.77	10.22	-1.73	13.08	-9.03	-12.11
Cone-shaped (1)	40	-3.72	6.50	1.82	41.82	6.69	-17.24
Cone-shaped (1)	60	-5.80	10.21	-0.91	59.78	-19.91	-0.58
Cone-shaped (2)	20	-5.99	5.09	-3.87	136.02	4.42	3.79
Cone-shaped (2)	40	-6.39	9.52	-3.22	88.30	-8.82	-7.20
Cone-shaped (2)	60	-5.90	10.36	-2.41	23.26	-13.46	-4.87
Cone-shaped (3)	20	-6.00	9.95	-2.24	43.79	-2.23	-4.91
Cone-shaped (3)	40	-5.10	10.66	-2.23	2.94	0.87	-6.97
Cone-shaped (3)	60	-5.35	9.68	-1.16	36.99	2.14	-1.34

In Table 1 we can compare results from each barrel itself and between them and from this it is evident that the difference in the gripping of the barrel to the weapon case has an influence on the position of the barrel muzzle when the bullet leave its.

Moreover it is also evident that the additional accessories have an influence on the barrel muzzles position which is also different at with all three different grippings. From Table 1 we cannot see the behavior of the barrel and the bullet during firing. Therefore Figures 3-5, 7-8, 10-11 and 13-14 show the courses of the barrel muzzle behavior at the presented node during the firing for each stated barrel and for the three different grippings. Figures 3, 7, 10 and 13 show the displacements of the barrel muzzle at node 10 648 in *x*, *y*, *z*-axis.

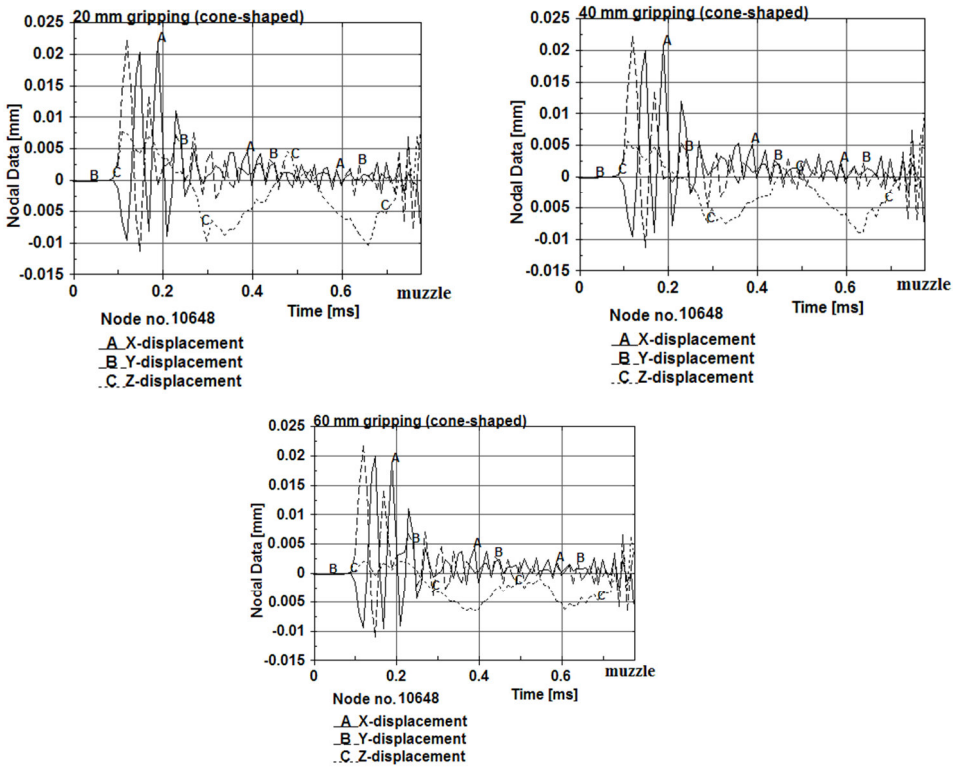

Fig. 3. Displacement of the barrel muzzle at node 10 648 in *x*, *y*, *z*-axis of the simple cone-shaped barrel at three different grippings

Figure 4 shows the results of acceleration of the barrel muzzle only for the simple cone-shaped barrel, where we can see how the barrel muzzle is excited to the vibration when the bullet leaves the barrel muzzle. This vibration can have an influence on the following shots.

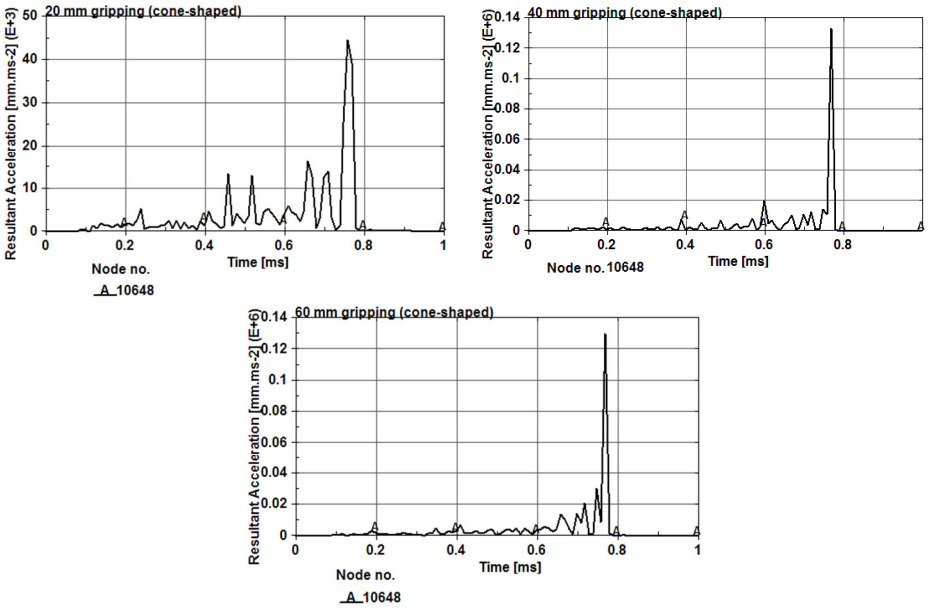

Fig. 4. Resultant acceleration of the barrel muzzle at node 10 648 of the simple cone-shaped barrel at three different grippings

In Fig. 5, 5a, 8, 11 and 14 displacements of the bullet base at node 26 703 in *x*, *y*-axis from 0 to 0.7765 ms when the bullet leaves barrel muzzle also for three different gripping for each barrel are shown.

In Fig. 6, 9 and 12 the cone-shaped barrels which each of them having being equipped with additional accessories, which have an influence on the barrels behaviour during firing are shown.

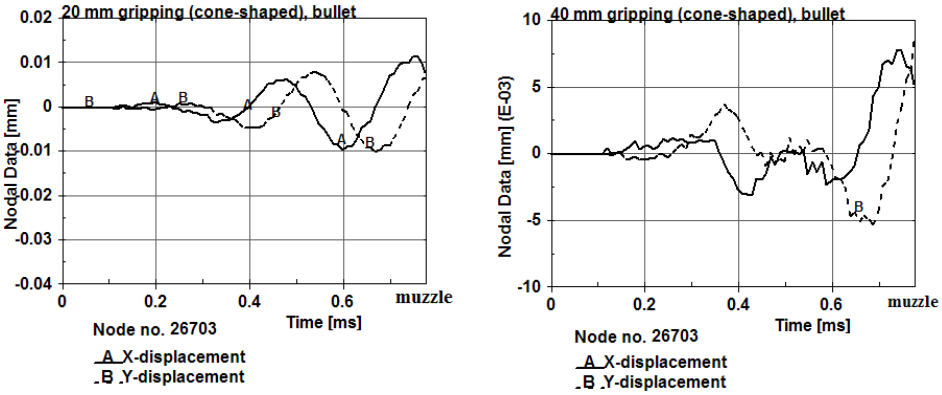

Fig. 5. Displacement of the bullet at node 26 703 in *x*, *y*-axis at the barrel muzzle of the simple cone-shaped barrel at 20 mm and 40 mm grippings

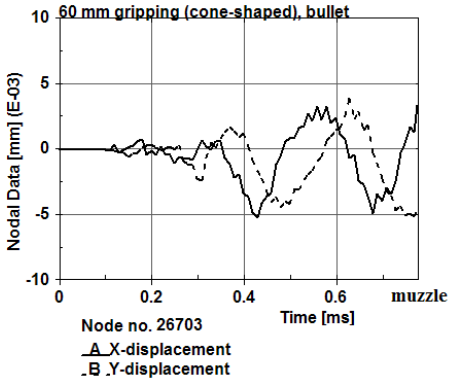

Fig. 5a. Displacement of the bullet at node 26 703 in *x*, *y*-axis at the barrel muzzle of the simple cone-shaped barrel at 60 mm gripping

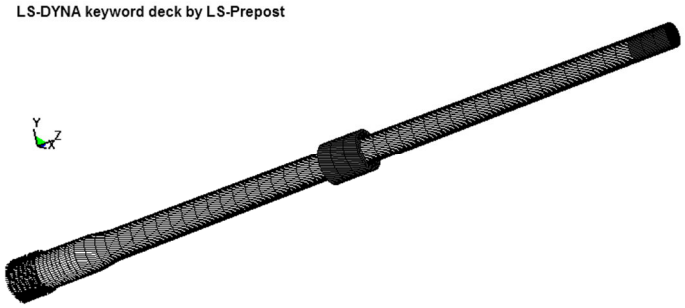

Fig. 6. Cone-shaped barrel (1) at 20 mm gripping (to the left) with additional accessories

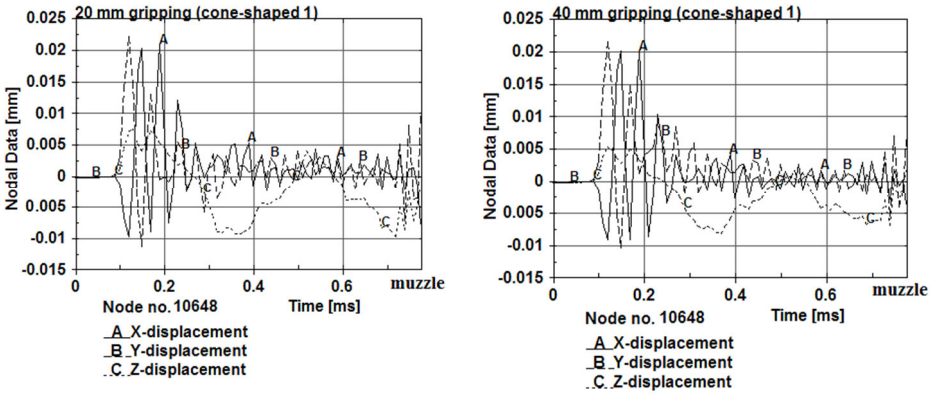

Fig. 7. Displacement of the barrel muzzle at node 10 648 in *x*, *y*, *z*-axis of the cone-shaped barrel (1) at 20 mm and 40 mm grippings

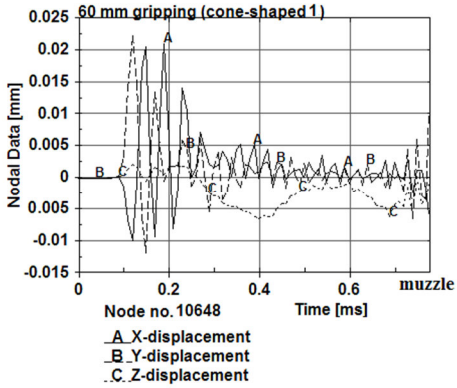

Fig. 7a. Displacement of the barrel muzzle at node 10 648 in *x*, *y*, *z*-axis of the cone-shaped barrel (1) at 60 mm gripping

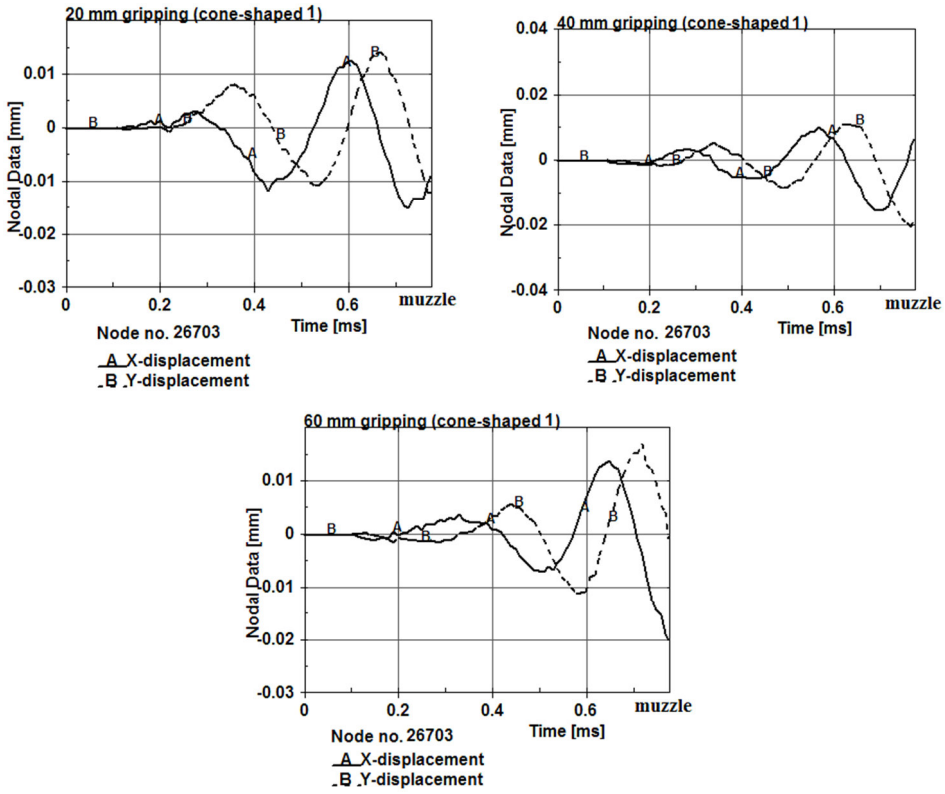

Fig. 8. Displacement of bullet at node 26 703 in *x*, *y*-axis at the barrel muzzle of the cone-shaped barrel (1) at three different grippings

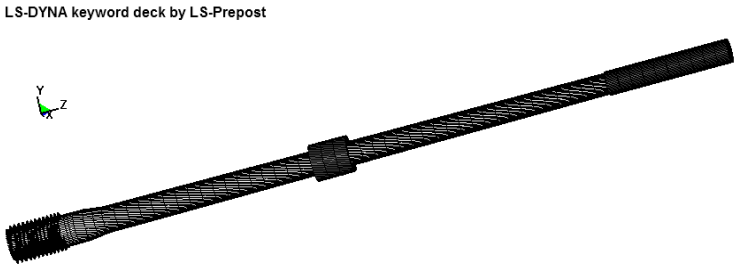

Fig. 9. Cone-shaped barrel (2) at 40 mm gripping (to the left) with additional accessories

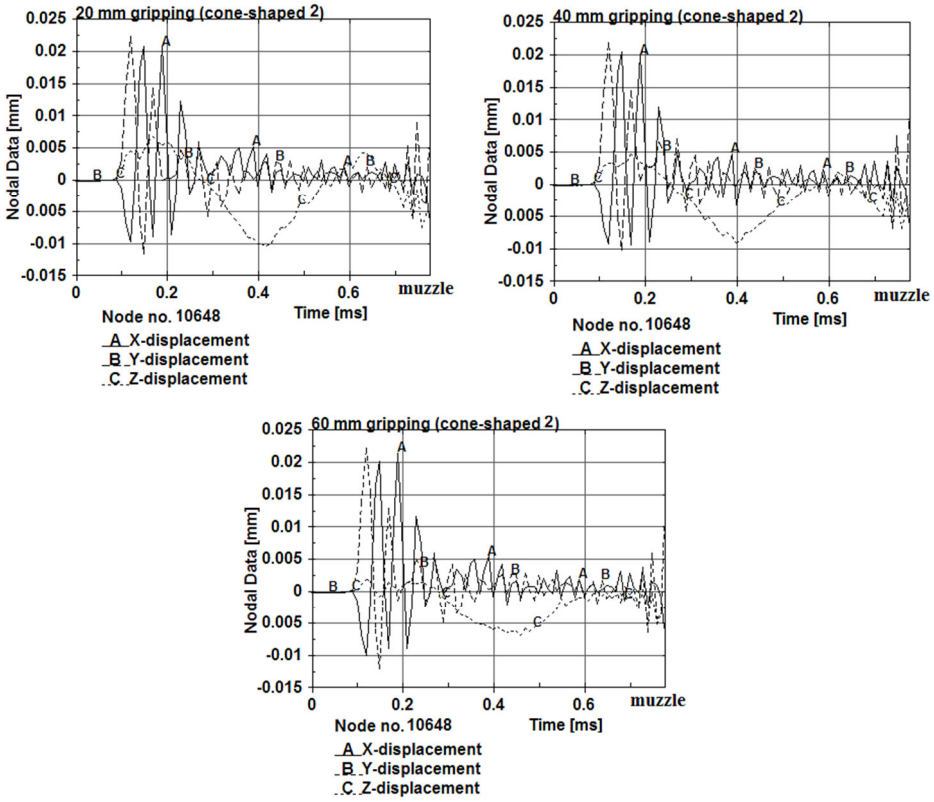

Fig. 10. Displacement of the barrel muzzle at node 10 648 in *x*, *y*, *z*-axis of the cone-shaped barrel (2) at three different grippings

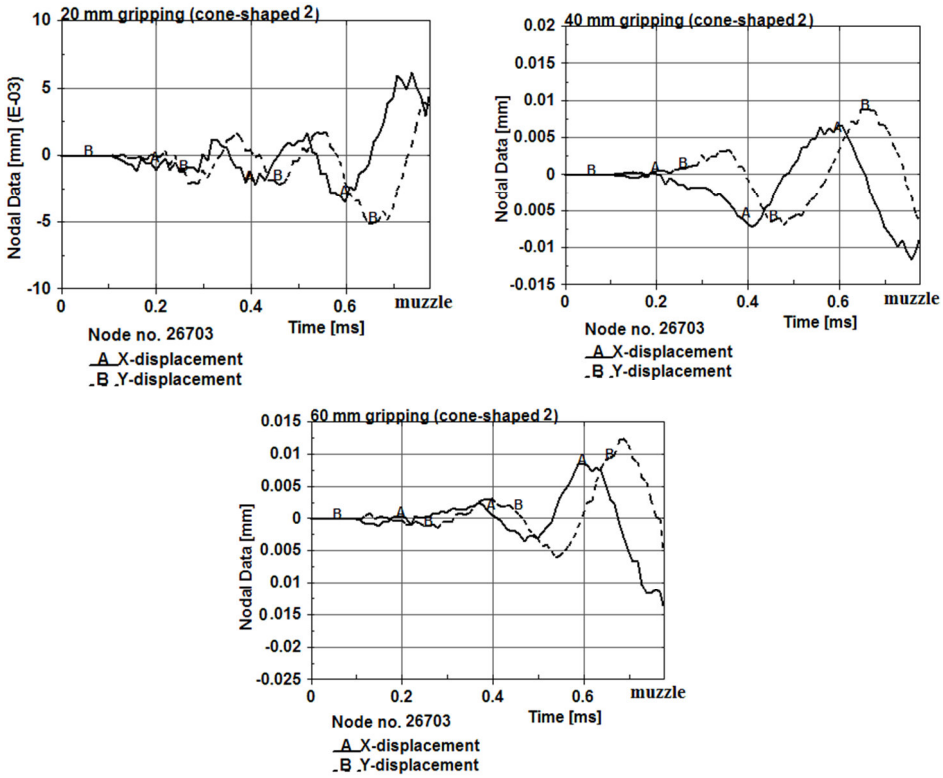

Fig. 11. Displacement of bullet at node 26 703 in *x*, *y*-axis at the barrel muzzle of the cone-shaped barrel (2) at three different grippings

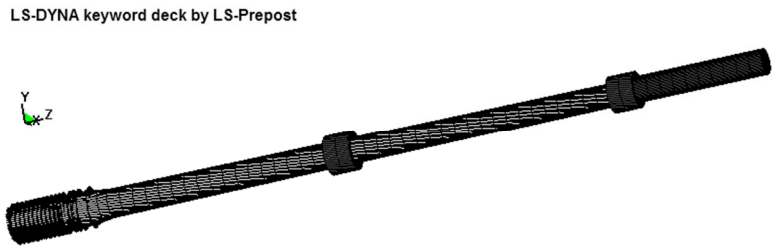

Fig. 12. Cone-shaped barrel (3) at 60 mm gripping (to the left) with additional accessories

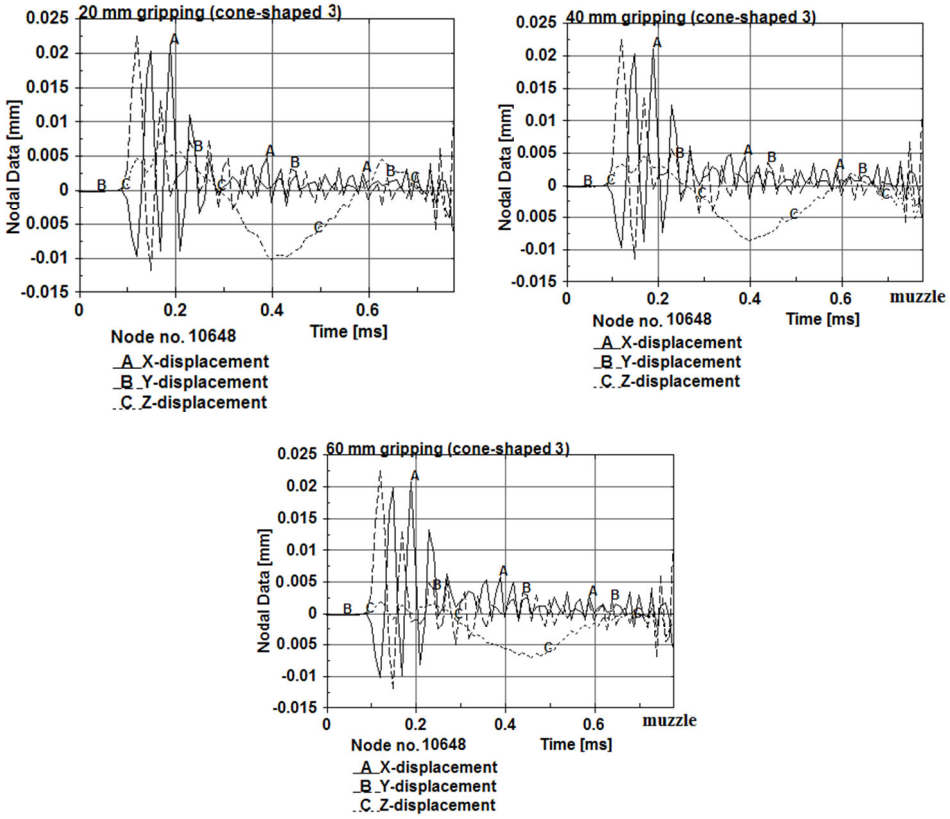

Fig. 13. Displacement of the barrel muzzle at node 10 648 in *x*, *y*, *z*-axis of the cone-shaped barrel (3) at three different grippings

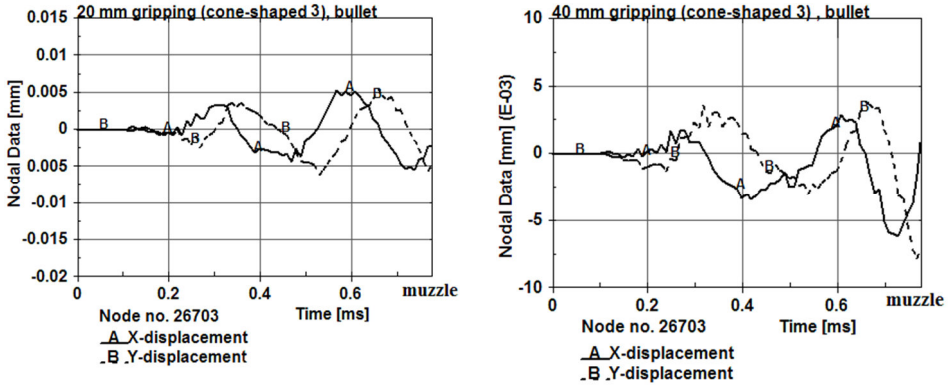

Fig. 14. Displacement of bullet at node 26 703 in *x*, *y*-axis at the barrel muzzle of the cone-shaped barrel (3) at 20 and 40 mm grippings

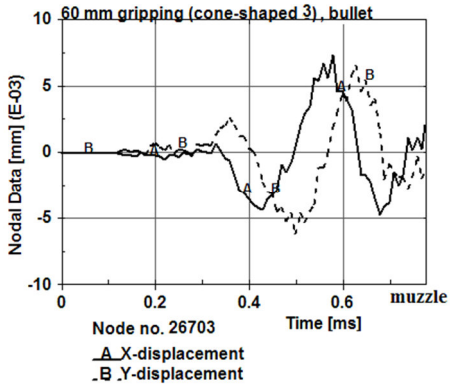

Fig. 14a. Displacement of bullet at node 26 703 in *x*, *y*-axis at the barrel muzzle of the cone-shaped barrel (3) at 60 mm gripping

The diferencies are more evident in Fig. 15÷18. Here it is clearly shown how the variation of conditions (different grippings and different added weight on the same barrel) can change the barrel muzzle position, which has an influence on the bullets flight path. For a better view of the bullets deviation from the barrel axis was made simulation at 10 ms.

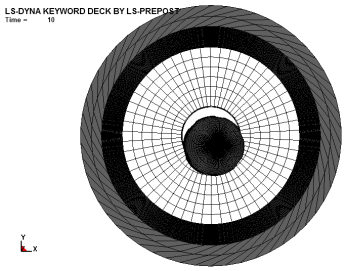

Fig. 15. Simple cone-shaped barrel at gripping 20 mm, deviation at 10 ms time flight of bullet

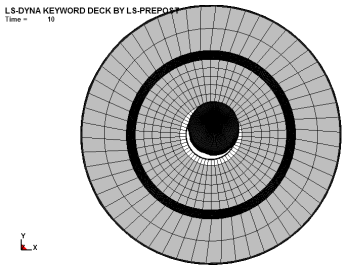

Fig. 16. Cone-shaped barrel (1) at gripping 40 mm, deviation at 10 ms time flight of bullet

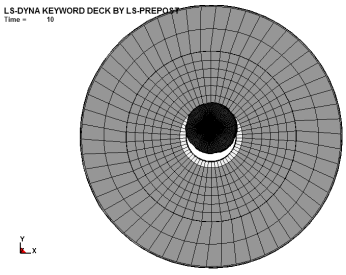

Fig. 17. Cone-shaped barrel (2) at gripping 40 mm, deviation at 10 ms time flight of bullet

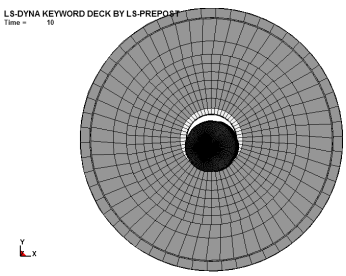

Fig. 18. Cone-shaped barrel (3) at gripping 60 mm, deviation at 10 ms time flight of bullet

4. CONCLUSION

A simple barrel and barrels with their accessories and bullet by finite element model in LS-DYNA are modeled. The aim was to obtain the results concerning the behaviour of the barrel during initial firing under ideal conditions. The ideal conditions means, that the barrel is perfectly straight without any manufacturing deviations, the same bullet is also without any shape or weight deviations and both the barrel and bullet are axial symmetrical. This simulation was also conducted without any temperature changes during the firing and without any influence on the barrel by the shooter. That means that the simulation only solved self-configuration weapon which is given by technology. The simulation at 10 ms was made for obtaining the bullets flight without any influence on gravity or wind, i.e. without external conditions. These all means, that we investigated the internal conditions of contact between the barrel and bullet with the real course of gunpowder gasses at three different grippings at the back of the barrel and around its chamber, which simulated gripping the barrel to the weapon case.

From the results listed in Table 1 and figures which represent the courses of various parameters we can say, that:

- both applied pressure and the movement of the bullet along the barrel gives rise to the barrels vibration, which has a significant influence on the bullets flight path when the bullet leaves the barrel muzzle;
- the length of the barrel gripping to the weapon case also has an influence to the barrels vibration and this changes the barrels muzzle position, which has an additional influence on the bullets flight;
- the combination of the additional accessories also has an influence on the barrels vibration and this changes the barrels muzzle position, which also has an additional influence on the bullets flight;
- the proper combination we can choose the combination, which will be has the smallest influence to the position on the barrel muzzle when bullet leaves it due to by technology.

REFERENCES

[1] Schwinkendorf K.N., Roblyer S.P., Three river technologies – Simulation of the vibrational response of a rifle barrel during firing, *Advanced Simulation Technologies Conference (ASTC '98)*, p. 66, 1998.

[2] Vítek R., Influence of the small arm barrel bore length on the angle of jump dispersion, *Proceedings of the 7th WSEAS International Conference on System Science and Simulation in Engineering – ICOSSSE '08* Wisconsin, p. 114, 2008.
http://www.vni.com/books/appstudies/rifle/rifle4.html.

[3] Varmint A., *FEA Rifle Barrel Dynamic Pressure Analysis of a 6PPC with and without a Tuner*, 2013. http://varmintal.com/apres.htm.
[4] *Impact Shift with a Suppressed Kalashnikov Action M62 Assault Rifle*. http://guns.connect.fi/rs/impact.html.
[5] Lisý P., Štiavnický M., Influence of the barrel oscillations into accuracy of small arms, *Proceedings of International Conference on Military Technologies*, Brno, pp. 1737-1744, 2011.
[6] http://world.guns.ru/assault/rus/ak-101-e.html.
[7] *LS-DYNA Theory Manual, Version 971*. Livermore Software Technology Corporation, March 2006.
[8] Bathe K.J., *Finite Element Procedures in Engineering Analysis*, Pretince Hall, 1982.
[9] *LS-DYNA Keyword User's Manual, Version 971*. Livermore Software Technology Corporation, January 2013.